ISSN 2072-5981
doi: 10.26907/mrsej

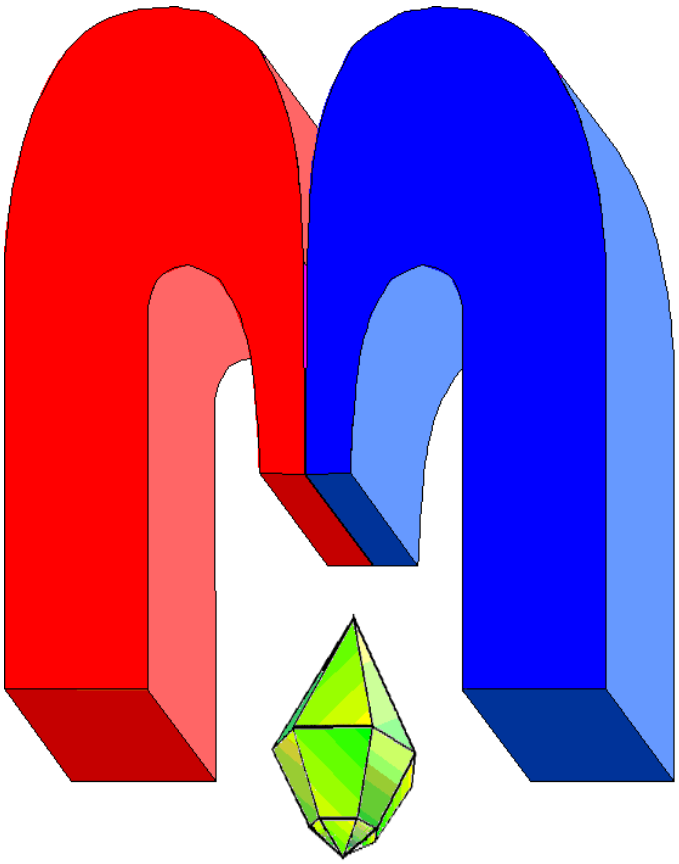

Magnetic Resonance in Solids

Electronic Journal

Volume 27
Issue 3
Article No ***25307***
1-13 pages
2025
doi: **10.26907/mrsej-25307**

http://mrsej.kpfu.ru
http://mrsej.elpub.ru

Established and published by Kazan University*
Endorsed by International Society of Magnetic Resonance (ISMAR)
Registered by Russian Federation Committee on Press (#015140), August 2, 1996
First Issue appeared on July 25, 1997

"***Magnetic Resonance in Solids. Electronic Journal***" (**MRS*ej***) is a peer-reviewed, all electronic journal, publishing articles which meet the highest standards of scientific quality in the field of basic research of a magnetic resonance in solids and related phenomena.

Indexed and abstracted by
Web of Science (ESCI, Clarivate Analytics, from 2015),White List (from 2023) *Scopus* (Elsevier, from 2012), *RusIndexSC* (*eLibrary*, from 2006), *Google Scholar*, *DOAJ*, *ROAD*, *CyberLeninka* (from 2006), *SCImago Journal & Country Rank*, etc.

Technical Editor
Maxim **Avdeev** (KFU, Kazan)
mrsej@kpfu.ru

* Address: "Magnetic Resonance in Solids. Electronic Journal", Kazan Federal University; Kremlevskaya str., 18; Kazan 420008, Russia

† In Kazan University the Electron Paramagnetic Resonance (EPR) was discovered by Zavoisky E.K. in 1944.

Application of complex NMR analysis to characterize pore space

D.S. Ivanov*, D.L. Melnikova, A.S. Alexandrov, V.D. Skirda

[1]Kazan Federal University, Kazan 420008, Russia

**f.ma.dima@mail.ru*

(received November 25, 2025; revised December 6, 2025; accepted December 8, 2025; published December 16, 2025)

Using the example of a study on a solid natural porous material, such as the core of dolomite rock, the effectiveness of three complementary NMR techniques is demonstrated. These techniques allow for the determination of the characteristics of the porous structure with sufficient accuracy, including the pore size distribution. Based on the combination of classical NMR relaxation and DDIF techniques, a method has been proposed for determining the surface relaxation parameter of the studied object without the need for additional physico-chemical research or reference to literature data.

PACS: 71.70.Ch, 75.10.Dg, 76.30.Kg, 71.70.Ej.

Keywords: magnetic resonance, NMR, relaxation, diffusion, porous media, pore size distribution, surface relaxation.

1. Introduction

The current understanding of solid materials is based on a deep and comprehensive analysis of experimental studies. Porosity plays a special role among the parameters that characterize a solid. Due to their unique properties, porous solid materials can be used in various technologies, such as batteries development and chemical catalysis. Various methods are used to study the characteristics of porous solid materials. To determine a relatively simple parameter like open macroporosity, techniques such as light microscopy, thermoporeometry, liquid volumetry and gas volumetry can be employed [1, 2]. Standard methods for characterizing the pore space in porous materials, such as mercury porometry, gas adsorption and computed tomography (CT), have significant limitations. These include destructiveness and indirect determination of pore sizes, as well as a narrow dynamic range. Other methods, such as those described by Dullien [3], Rouquerol [4] and Orlinskii [5], offer alternative approaches to characterizing porous materials. However, these methods also have limitations that need to be considered when selecting the most appropriate technique for a particular application [6]. At the same time, mercury porometry, which is considered the gold standard for determining porosity, has the disadvantage of using toxic reagents and the risk of damaging the fragile rock structure due to high pressure. While adsorption isotherms and several other methods provide general information about the pore structure, nuclear magnetic resonance (NMR) allows for spatially selective analysis, allowing us to distinguish between pores of different sizes and shapes and their contribution to the overall behavior of the system.

In the article [7], the main focus is on the characterization of porous materials using NMR techniques. The review not only discusses the traditional NMR spectroscopy methods, but also explores relaxation time measurement techniques used to characterize porous solids. Additionally, it examines the effects of adsorbate interactions with the solid surfaces of pores. The review also explores the use of pulsed field gradient (PFG) techniques, which are primarily used to study transfer characteristics. Furthermore, it considers the potential of more complex techniques such as magnetic resonance imaging (MRI) for characterizing porous materials. In the paper [8], the

possibility of obtaining information about the pore size distribution of aerogel from spin-lattice relaxation data of introduced ^{3}He is demonstrated.

A sufficiently high reliability and stability of the measured spin-spin relaxation time spectra (T_2) for characterizing the pore structure of natural low-permeability porous materials was demonstrated in [9–11]. However, this requires verification of NMR data in combination with other petrophysical properties and macroscopic characteristics obtained by other physical and chemical methods.

In this paper, we aim to demonstrate the potential of combining several relatively simple techniques using a single research method − the NMR method.

The simplest methods for characterizing porous structures include measurements of spin-spin (T_2) and/or spin-lattice (T_1) relaxation times. Under certain conditions, these relaxation times can be directly related to the characteristics of the porous space. For example, for T_2 relaxation times (the most common type of measurement in NMR practice), there is a simple relationship with pore sizes (r):

$$\frac{1}{T_2} = \frac{\rho S}{V} = \frac{3\rho}{r}, \tag{1}$$

where ρ is the surface relaxivity and $S/(V)$ is the ratio of the surface area of the pore space to its volume, also known as the specific surface area.

The most attractive use of expression (1) is in cases where the recorded relaxation time spectrum is directly related to the pore size spectrum. This approach is valid under the assumption of isolated pores, but a number of studies confirm its validity [12,13]. However, it has been shown that a type (1) bond may not always accurately reflect the real characteristics of porous materials, especially in the nanometer range. This is due to the averaging of relaxation times caused by diffusion between pores and the poor sensitivity of the method to pore geometry. Therefore, according to [14], the use of this expression may lead to large errors in the estimation of small pore sizes [15]. Several analytical models are presented in [16] to account for the influence of connectivity between pores on the distribution of relaxation times. The issues associated with strong inhomogeneous magnetic fields occurring in porous media due to variations in magnetic susceptibility at solid/liquid interfaces and intrinsic or artificially introduced magnetic impurities are discussed in [17, 18]. An important consequence of these magnetic field gradients is the necessity to consider the contribution of diffusion to transverse relaxation, which is a challenging task [19, 20] .

It should be noted that many factors influence the process, such as the roughness of the pore surface, the presence of internal gradients, and the shape of the pores. These factors can be accounted for by making some adjustments to the surface relaxation value in equation (1). However, one major challenge is that when studying natural porous materials, the surface relaxation coefficient can be unknown. The standard method for obtaining surface relaxation values today is to calculate them based on comparing nuclear magnetic resonance (NMR) data with mercury porometry, low-temperature nitrogen adsorption, and using the Kozeni-Karman equation [21]. However, there is often a lack of consistency between the results obtained using different methods, even when studying the same type of porous material.

In the work by Zhao P. et al. [22], it was shown that the value of the surface relaxation parameter determined using the Kozeni equation is greater than the values obtained using mercury porometry and low-temperature nitrogen adsorption. At the same time, the range of surface relaxation values for dolomite from one rock sample varies from 3.41 to 40 μm/ms.

Similarly, in the study by Rogozin A. et al. [23–26], the values of the relaxation parameter ρ range from 0.1 to 1.6 μm/ms for samples of similar dolomite rocks. Thus, even for samples of the same type, a fairly wide range of values for the surface relaxation parameter can be found, which confirms the importance of the task of independently measuring this characteristic.

Another negative aspect of the nuclear magnetic relaxation method, as previously noted, is that expression (1) establishes a linear relationship between pore size and relaxation time only under the assumption of isolated pores. However, for cohesive pores, there are deviations from this linear dependence, as shown in the work [27]. These deviations will be more noticeable for small values in the pore size spectrum, where diffusion averaging effects are more pronounced. The problem of studying small pores can be solved by using the NMR cryoporometry technique, which has been developed based on the works [28–30]. This technique is based on the Gibbs-Thomson effect, which describes the dependence of a crystal's melting point on the curvature of its interface. This effect leads to a decrease in the melting point of the liquid in a porous medium, as described by the following equation:

$$\Delta T = T_0 - T(r) = \frac{k_{\mathrm{GT}}}{r}, \tag{2}$$

where T_0 is the normal melting point, $T(r)$ is the melting point of a crystal in a pore with radius r, and k_{GT} is the Gibbs-Thomson constant, which takes into account the surface energy at the liquid-solid interface. The value of this constant, for example, for water was determined in work [31] and is equal to 49-58 nm*K. In the case of hydrocarbons, such as benzene, $k_{\mathrm{GT}} =$ 110 nm*K has been found. Note that the characteristics of spin-spin relaxation depend strongly on the state of matter aggregation. Thus, for a liquid (molten) fluid, typical T_2 relaxation times are in the range of 0.1 second or more, for example for water. At the same time, the T_2 relaxation time for the solid (ice) state is estimated to be 10 μs. Thus, it is not difficult to isolate the fraction (P_{s}) of the total NMR signal, which quantitatively characterizes the relative content of the crystalline component in the fluid. By recording the NMR signal as a function of temperature, we can construct the dependence $P_{\mathrm{s}}(T)$, which reflects the features of the phase transition in the porous medium due to the effect of pore size on the melting temperature, in accordance with equation (2). The transformation from the experimentally measured $P_{\mathrm{s}}(T)$ dependence to the pore size can be carried out using the well-known Strange-Rahman-Smith transformation [28].

Cryoporometry does not require calibration with other methods because it does not depend on the value of ρ. This makes it an exceptionally valuable tool for accurately characterizing nano- and mesoporous materials (from 20 to about 100 nanometers), where traditional NMR relaxometry can introduce systematic errors [32]. Unfortunately, the cryoporometry technique becomes less effective for larger pore sizes due to its inability to accurately measure small differences in temperature (ΔT).

In order to overcome the limitations of the cryporometry method and techniques that assume a direct relationship between relaxation time and pore size, more sophisticated experimental approaches are proposed. These include investigating the T_2-T_2 correlation [33] or the correlation between relaxation times and self-diffusion coefficients. To measure self-diffusion coefficients, significant modifications to NMR equipment are typically required to provide adjustable external magnetic field gradients.

One such method that has been proposed is the DDIF (Diffusion Decay in Internal Field) technique [34], which allows for the estimation of pore size through the analysis of relaxation

in inhomogeneous internal magnetic fields at the rock-fluid interface. The key works that lay the foundations for this methodology include [35] and [36]. The DDIF methodology is based on several considerations. When a fluid molecule wanders through a pore, it acquires a random precession phase due to the action of the nonlinear internal magnetic field gradient inside the pore. This leads to non-relaxation decay of the NMR signal. When the molecule enters an adjacent pore, the dephasing process starts anew in the gradient field of the new pore. If neighboring pores are similar in size, their average internal gradient values will also be similar. This results in the diffusion contribution to relaxation being the same for molecules that remain in the initial pore and those that move into the neighboring pore. In other words, the contribution of diffusion to relaxation is limited by time at which the path taken by molecules during diffusion becomes comparable to the size of a single pore, whether it is an isolated pore or not. Therefore, the key aspect of the DDIF method is to determine a diffusion time that meets this condition.

$$r = \sqrt{6 D_{\mathrm{s}} \tau_{\mathrm{d}}(r)}, \tag{3}$$

where D_{s} is the diffusion coefficient, τ_{d} is the diffusion time, and r is the pore size. An experimental indication of the fulfillment of condition (3) is the establishment of the fact that the influence of internal magnetic field gradients on the NMR signal amplitude is independent at all times greater than $\tau_{\mathrm{d}}(r)$. It is clear that in the case of pore size distribution, finding such a diffusion time after which the influence of internal gradients becomes vanishingly small will correspond to the fulfillment of relation (3) for maximum pore size.

Obviously, each of the listed NMR techniques has both advantages and limitations. Nevertheless, it is hoped that their combination will make it possible to compensate for the disadvantages of each of the methods and obtain information about the characteristics of the porous space of porous materials without the need to use other physicochemical methods.

2. Materials and research methods

For this research, a sample of natural porous dolomite rock was chosen. By the data from [37] the sample may contain pores with sizes in range from nanometers to tens of micrometers. The sample was cut into a 9.5 mm cylinder to fit into a 10 mm tube. After this in order to remove all residual water the sample was pre-dried until the sample mass stays contant and there was no NMR signal from dried sample. Depending on the experiment, the sample could be saturated with either double-distilled water or chemical pure brand benzene for cryoporometry experiments. Saturating dry cores with liquid was done under reduced external pressure, following the recommendations in GOST 26450.1-85. The porosity of the sample was 8%.

All the experimental studies described in this paper were conducted on the "Proton 20M" NMR relaxometer (by "Chromatech" inc.) with a resonance frequency of ^{1}H 22.5 MHz and the ability to adjust the temperature with an accuracy of 0.1 K. The "dead time" (time interval immediately after an RF pulse where the receiver is unable to detect the signal) of the probe is 11 μs. All acquired relaxation attenuation data were processed using the OriginLab software. The spectra of longitudinal and transverse relaxation times were derived from the experimentally obtained relaxation attenuation curves using the Spectrum of Spin-Spin Relaxation Times program, developed at the Department of Physics of Molecular Systems at the Institute of Physics at KFU. Further details regarding the acquisition of experimental data can be found in the relevant subsections of the paper [38].

2.1. NMR relaxometry

To implement the pore determination technique based on NMR relaxometry data, the standard Carr-Purcell-Meiboom-Gill [39] pulse sequence was used. The measurements were carried out with delay 2τ between π-pulses equals 100 μs and at sample temperature of 298 K. The relaxation decays obtained were approximated by an integral sum of exponential terms with spin-spin relaxation times and fractions, according to the following formula:

$$A(t) = \int_0^\infty f(T_2)\, e^{-\frac{t}{T_2}}\, dt, \tag{4}$$

where $A(t)$ represents the NMR signal measured in a CPMG sequence and $f(T_2)$ is the amplitude distribution function for spin-spin relaxation times (T_2).

2.2. NMR cryoporometry

For NMR cryoporometry experiments, the core sample was saturated with chemically pure benzene, which has a melting point of 278.5 K. The experiment consisted of several stages, including "freezing". The sample temperature was lowered directly in the NMR sensor to 252 K, corresponding to a supercooled temperature of more than 25 degrees below the melting point. This high degree of supercooling ensured a fast crystallization process, with a crystallinity of at least 99%. The sample temperature in the NMR sensor was then increased stepwise by 1 K over 20 minutes, up to about 275 K. At higher temperatures, the step size was reduced to 0.1 K, and the hold time at each step increased to 60 minutes [40]. This procedure was repeated twice: once for a volume of benzene, and once for a core sample with pores filled with benzene. At each temperature step, a solid-echo signal was recorded, which made it possible to compensate for the effect of dead time after the 90th pulse. This actually corresponded to the registration of the FID signal starting from zero time. The Solid-Echo pulse sequence ($\tau = 12\,\mu$s) was used for the research [41,42]. The recorded relaxation decay was approximated by an expression like:

$$\frac{A(t)}{A(0)} = P_\mathrm{s} e^{-\frac{t^2}{T_{2\mathrm{s}}^2}} + \sum p_\mathrm{i}\, e^{-\frac{t}{T_{2\mathrm{i}}}}, \tag{5}$$

where P_s is the population of the solid–state (Gaussian) component; $T_{2\mathrm{s}}$ is the time of transverse relaxation of the solid–state component; p_i are the relative fractions of the components characterized by relaxation times $T_{2\mathrm{i}}$ (relating to liquid (molten) phase of the fluid inside the porous space); $P_\mathrm{s} + \sum p_\mathrm{i} = 1$.

The main objective of the experiment was to establish differences in the temperature dependences $P_\mathrm{s}(T)$ for the fluid in the volume and for the fluid in the porous structure of the sample in the slow heating mode in the range from 252 to 280 K, including the areas of crystallization and melting of the liquid. Benzene of the chemical pure brand with a melting point of 278.5 K was used as a fluid in cryoporometry experiments.

2.3. DDIF Methodology

The Diffusion-Driven Internal Field (DDIF) technique is based on the use of internal magnetic field gradients within a porous medium containing a liquid [43]. Two sequences were employed in the experiments: a DDIF sequence that records the attenuation of the spin echo signal due to internal magnetic field gradients (Figure 1A), and an inversion-recovery sequence followed by formation of a spin echo signal (Figure 1B). It should be noted that the DDIF sequence is actually a well-established sequence of stimulated echoes. In contrast to the PFG NMR experiments [44],

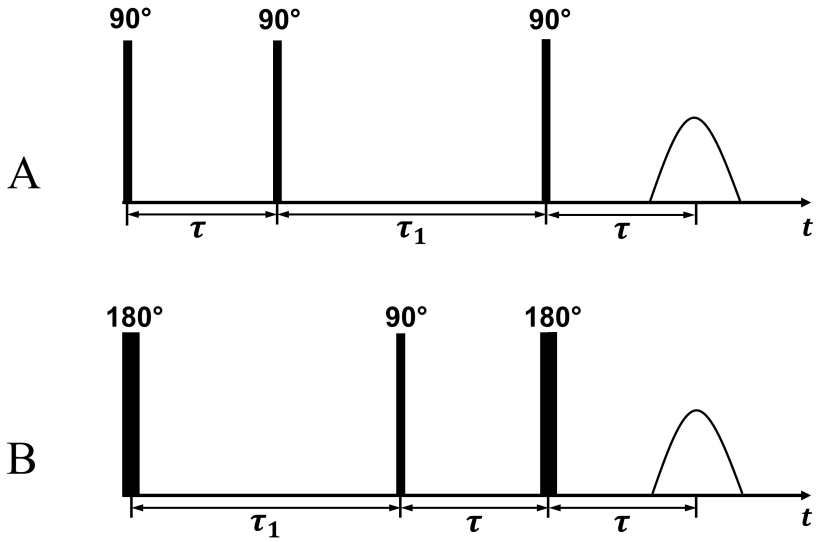

Figure 1. Pulse sequences: A – DDIF, where the internal gradients of the magnetic field act in time intervals indicated by τ. B – The "inversion-recovery" sequence with an echo signal.

the echo signal in the DDIF sequence is affected only by internal and generally nonlinear but constant in time magnetic field gradients caused by differences in magnetic susceptibility values for the porous substance and the intrapore space. A notable feature of this sequence is that these internal gradients affect the amplitude of the echo signal only during specific time intervals τ. This allows for adjusting the value of τ so that the gradients have a significant impact on the amplitude of the stimulated echo. By varying the time interval τ_1, the diffusion time $\tau_\mathrm{d} = \tau_1 + 2/3\tau$ can be effectively changed, thus setting the scale for spatial displacements of fluid molecules. The second sequence, called the "inversion-recovery" sequence, was used to measure the contribution of spin-lattice relaxation and then exclude it from the results obtained using the DDIF sequence. In both sequences, the values of the time interval τ were set to be the same. Note that the dependence of the echo amplitude $A_\mathrm{E}(\tau, \tau_\mathrm{d})$ on the diffusion time τ_d, recorded in this way, contains an additional contribution due to spin-lattice relaxation in addition to the desired diffusion attenuation caused by the movement of molecules in an inhomogeneous magnetic field. To determine this contribution and then exclude it, it is necessary to conduct independent studies of spin-lattice relaxation, for example, using the "inversion-recovery" technique. In order for the experimental data in this sequence to match the DDIF experiment as much as possible, we used the sequence shown in Figure 1B. The relaxation decay function $A_\mathrm{R}(\tau, \tau_\mathrm{d})$ was determined from the experimentally measured dependence of the amplitude of the spin echo signal on the time interval t_1 in this sequence. In this case, the value of τ was set equal to the corresponding value in the DDIF sequence. Then, the result of normalizing the experimentally measured $A_\mathrm{E}(\tau, \tau_\mathrm{d})$ function to the spin-lattice relaxation function $A_\mathrm{R}(\tau, \tau_\mathrm{d})$ will be the desired $A_\mathrm{E}(\tau, \tau_\mathrm{d})/A_\mathrm{R}(\tau, \tau_\mathrm{d})$ function, which can be used to determine the pore size distribution [43]. By analyzing this function, information about the pore size distribution can be obtained. In particular, the inverse Laplace transform can be used. In the long diffusion time region, it is expected that the $A_\mathrm{E}(\tau, \tau_\mathrm{d})/A_\mathrm{R}(\tau, \tau_\mathrm{d})$ function reaches a plateau (independent of τ_d), which means that the root-mean-square displacement of molecules becomes larger than the upper limit of the pore size distribution. Therefore, the DDIF method can be used to accurately determine this upper bound [45, 46]. It is important to note that the measurement result will not be influenced by factors such as the roughness of the pore surface, the presence of paramagnetic

impurities, or the values of surface relaxation.

3. Experimental Results and Discussion

A typical example of relaxation decay measured using the CPMG technique for a core sample of dolomite rock is shown in Figure 2. As can be seen in Figure 3, relaxation decay is

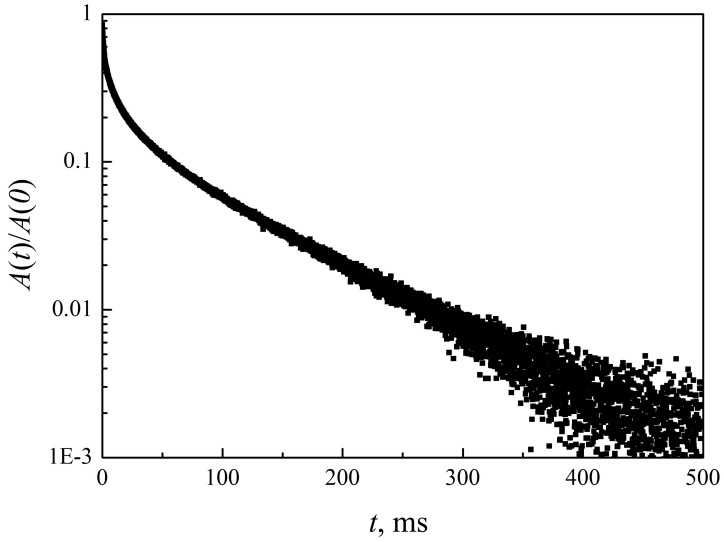

Figure 2. Relaxation decay, normalized to the amplitude at the initial time, obtained using the CPMG pulse technique for a core sample saturated with water. The temperature of the experiment was 293 K.

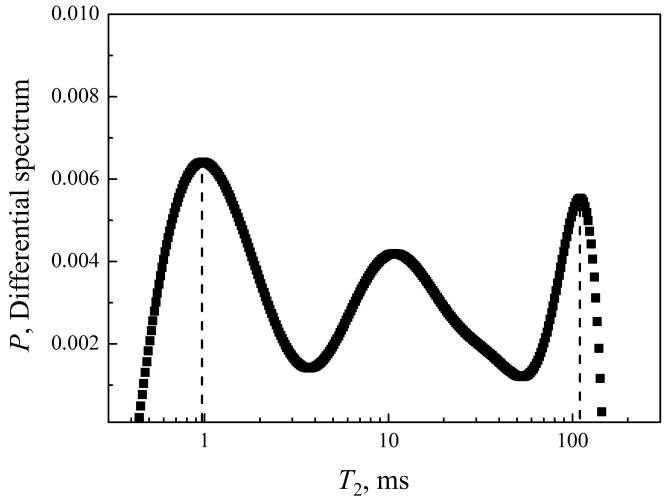

Figure 3. Differential spectrum of spin-spin relaxation times for a core sample saturated with water. The dotted lines conventionally indicate the upper (100 ms) and lower (1 ms) boundaries of the spectrum.

characterized by a pronounced non-exponential behavior. The result of converting relaxation decay into a spectrum of relaxation times using the program "Spectrum of Spin-Spin Relaxation Times" [38] is presented in Figure 3.

The relaxation time spectrum in the figure shows a fairly wide range of relaxation times, from

1 ms to 100 ms. Based on this, if we consider the applicability of equation (1), we should expect a similarly wide range of pore sizes in the material. However, to use this equation, we need information about the surface relaxation time, which should correspond directly to the porous material. Since this information is often not available, literature data or additional experiments, such as mercury porometry, are used. Let's try to address this issue using NMR data. We can use the DDIF sequence to obtain information about the maximum pore sizes. At least, this technique will allow us to associate the upper bound of relaxation times in the T_2 spectrum in Figure 3 with the upper bound of pore sizes. This can be done using the DDIF technique, as noted above.

Figure 4 shows the dependence of the echo amplitude $A_{\mathrm{E}}(\tau, \tau_{\mathrm{d}})$ for the DDIF sequence (Figure 1a) and the relaxation decay $A_{\mathrm{R}}(\tau, \tau_{\mathrm{d}})$, which characterizes the spin-lattice relaxation process. It also shows the result of normalizing $A_{\mathrm{E}}(\tau, \tau_{\mathrm{d}})$ by $A_{\mathrm{R}}(\tau, \tau_{\mathrm{d}})$, allowing us to take into account the contribution of spin-lattice relaxation to $A_{\mathrm{E}}(\tau, \tau_{\mathrm{d}})$. As we can see from Figure 4,

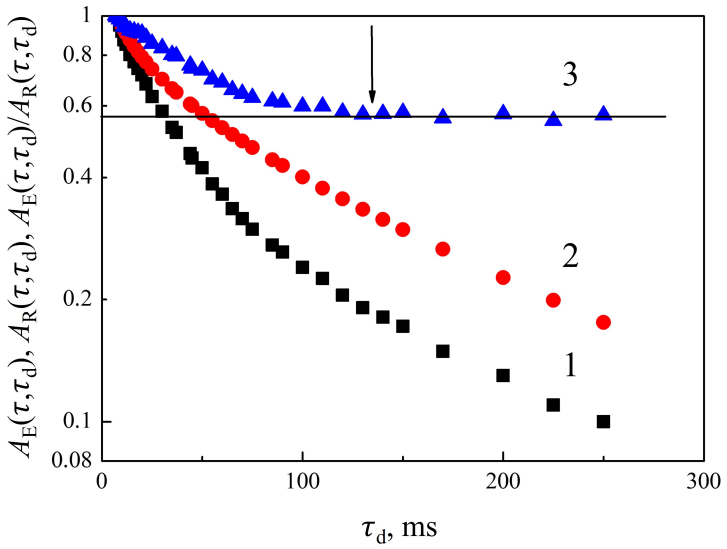

Figure 4. Dependence of $A_{\mathrm{E}}(\tau, \tau_{\mathrm{d}})$ – the amplitude of the stimulated echo - on the diffusion time in the DDIF sequence (curve 1), the relaxation decay $A_{\mathrm{R}}(\tau, \tau_{\mathrm{d}})$, which characterizes the spin-lattice relaxation process (curve 2), and the result of normalizing $A_{\mathrm{E}}(\tau, \tau_{\mathrm{d}})/A_{\mathrm{R}}(\tau, \tau_{\mathrm{d}})$ (curve 3). The arrow indicates the region where the effect of internal magnetic field gradients on the NMR signal amplitude becomes negligible. In both experiments $\tau = 8$ ms and the temperature was 293 K. All curves have been normalized to the initial amplitude.

after taking into account the contribution of spin-lattice relaxation (curve 2), the dependence of the echo amplitude in the DDIF sequence (curve 1) is transformed into a dependence (curve 3), demonstrating the output to a constant level for diffusion times greater than a certain critical value of about 100-150 ms. According to [43], it is this diffusion time that corresponds to the diffusion shifts corresponding to the upper boundary in the pore size distribution. Using the standard expression:

$$r = \sqrt{6 D_{\mathrm{s}} \tau_{\mathrm{d}}}, \tag{6}$$

with a diffusion time of 125 ms and a self-diffusion coefficient of 2.7 $10^{-9}\, m^2 s^{-1}$, the upper limit of the pore size is estimated at 45 microns.

If we take this result as a basis, then the upper limit ($\sim$ 100 ms) of the spin-spin relaxation time spectrum shown in Figure 3 corresponds to a pore size of about 45 microns. Given this, it can be assumed that for the sample under study, the surface relaxation can be described by

the value $\rho = 0.15\,\mu$m/ms. This value ρ does not contradict the data of [23], however, differs significantly from the estimates given in [22].

Assuming that expression (1) is valid for the entire range of relaxation times, it is easy to obtain a spectrum characterizing the pore size distribution in the object under study (Figure 5). So, according to the data presented in Figure 5, the lower limit of the pore size is in the range of

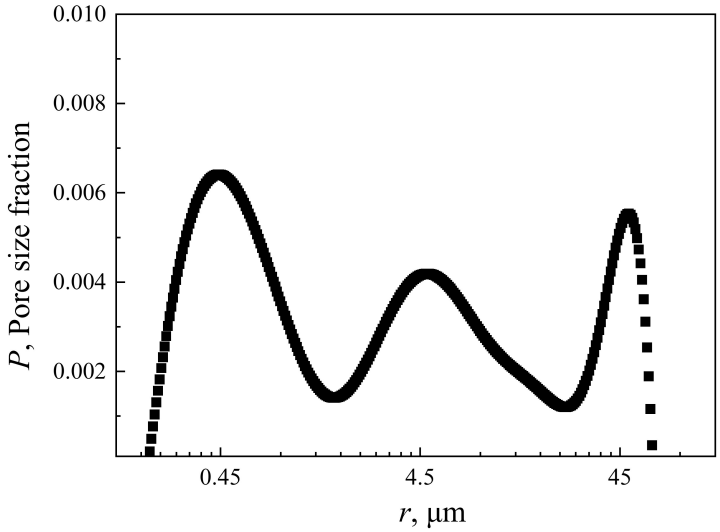

Figure 5. Pore size distribution, obtained by applying equation (1) to the spectrum of spin-spin relaxation times ($\rho = 0.15\,\mu$m/ms was used).

values on the order of $0.45\,\mu$m. This result was obtained by analyzing the spectrum of spin-spin relaxation times and using the value of $\rho = 0.15\,\mu$m/ms calculated from a comparison between relaxation data and data from the DDIF technique. However, this comparison between the two techniques was done in the upper limit regions of the T_2 time spectrum, and therefore, the pore sizes. If we consider the comments made in [14, 15, 17, 18], then the validity of applying (1) to the entire range of relaxation times and pore sizes remains uncertain. Therefore, it seems necessary to conduct additional experiments in order to verify the accuracy of the data presented in Figure 5. Specifically, it is important to focus on the lower end of the pore size range, from 0.45 microns and below.

In connection with the above, it seems reasonable to use the NMR cryoporometry technique. However, as previously noted, one of its main drawbacks is its poor sensitivity in detecting pores larger than 50-100 nm. This is due to the difficulty in registering values that are too small. For example, if we assume a pore size of 1 micrometer and water as the fluid inside the pore with $k_{\mathrm{GT}} \approx 50$ nm*K, the expected value of the melting point shift for water inside the pore would be only 0.05 K. However, if benzene were used instead of water with $k_{\mathrm{GT}} = 110$ nm*K [47], for pores with sizes around $0.45\,\mu$m (the lower limit of the r-spectrum according to the data in Figure 3), the expected temperature depression would be 0.25 K. To register these small changes the accuracy of sample temperature setting must be at least 0.1 K. An additional goal of this experiment could be to demonstrate the absence (or presence) of specific pores in the structure of a porous material. These pores may be too small to be detected in the relaxation time spectrum, as they would be averaged out due to the effects of self-diffusion on small spatial scales.

Figure 6 shows the evolution of the Solid-Echo signal for a benzene sample in a porous medium during heating process. Starting at 278.3 K, a 0.13 fraction of liquid-phase component appears

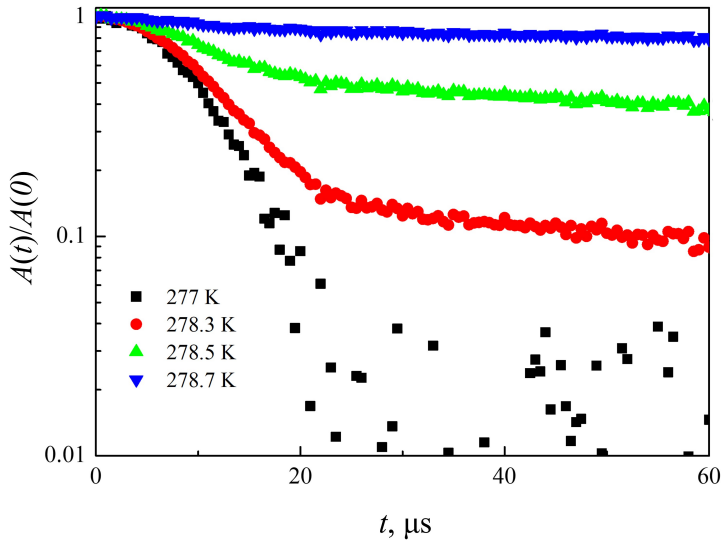

Figure 6. Evolution of Solid-Echo signal for a core sample saturated with benzene during heating process.

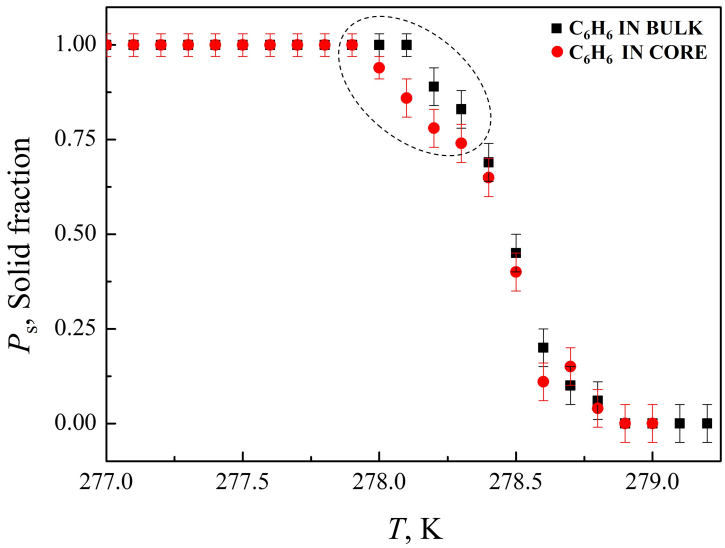

Figure 7. Temperature dependences of $P_s(T)$, the fraction of benzene molecules in the crystalline state, for a bulk sample (black symbols) and for a core sample saturated with benzene (red symbols).

in echo signal and fraction P_s of solid-phase decreases to 0.87 (according to eq. 5). As the temperature increases, the fraction of the solid-state component continues to decrease to 0.47 at 278.5 K and only 0.1 at 278.7 K. Spin-spin relaxation time T_{2s} of solid-phase remains unchanged approximately equals 10 μs. The temperature dependence of $P_s(T)$ determined from the analysis of the shape of the Solid-Echo signals is shown in Figure 7 for both samples, benzene in bulk and benzene with a porous core structure, under conditions of slow temperature increase.

The relaxation attenuation shown in Figure 6 clearly demonstrates the possibility of approximating it by an expression of the form (5), with the ability to determine the proportion of P_s that corresponds to the proportion of benzene molecules in the solid crystalline state.

As can be seen from Figure 7, only for the temperature range from 278.0 K to about 278.3 K in the range of the P_s fraction from 1 to 0.7 (see area enclosed by a dashed line in Figure 7), we can talk about a difference in the recorded $P_s(T)$ dependencies, indicating that for some (no

more than 30%) of the benzene molecules in the porous structure, melting occurs approximately 0.3 K at lower temperatures compared to the benzene sample in volume. For all other benzene molecules, there are no signs of differences in the $P_s(T)$ dependencies.

In general, the cryoporometry data fully confirm the information about the pore size distribution obtained above based on the data from nuclear magnetic relaxation and the DDIF technique. The region found on the $P_s(T)$ dependences, in which a melting temperature shift of about 0.3 K is recorded, correlates with the lower boundary in the pore size spectrum – values in the region of 0.5 microns. At the same time, it can be seen from the spectrum shown in Figure 5 that no more than 30-40% of the volume of the entire porous space corresponds to this region. The sizes of all other pores are characterized by significantly large values (from units to tens of microns), so that the values predicted according to (2) ΔT for them become too small for their registration.

4. Conclusion

The conducted research clearly demonstrates that it is impossible to obtain reliable information about the characteristics of porous structures and the pore surfaces (surface relaxation) of solid porous materials without an integrated analytical approach. Using isolated methods, such as computed tomography or mercury porometry, despite their power, often leads to fragmented or even contradictory information. However, the integration of classical NMR relaxometry data with DDIF techniques based on internal magnetic field gradients and cryoporometry makes it possible to obtain accurate information about pore size distributions.

The relaxivity (ρ) value is a parameter that reflects, in one way or another, the properties of the pore surface. In this regard, an important result of the study was the demonstrated possibility of directly determining the characteristics of surface relaxation by comparing the results obtained using two NMR techniques, without having to refer to other experiments or literature data, which may not correspond to the object under study.

Acknowledgments

This work was funded by the subsidy allocated to Kazan Federal University for the state assignment in the sphere of scientific activities number FZSM-2023-0016.

References

1. Danielson R., Sutherland P., *Methods of soil analysis: part 1 physical and mineralogical methods* **5**, 443 (1986).

2. Qiu J., Khalloufi S., Martynenko A., Van Dalen G., Schutyser M., Almeida-Rivera C., *Drying Technology* **33**, 1681 (2015).

3. Dullien F. A., Batra V., *Industrial & Engineering Chemistry* **62**, 25 (1970).

4. Rouquerol J., Avnir D., Fairbridge C., Everett D., Haynes J., Pernicone N., Ramsay J., *Pure and Applied Chemistry* **66**, 1739 (1994).

5. Galukhin A., Osin Y., Rodionov A., Mamin G., Gafurov M., Orlinskii S., *Magnetic Resonance in Solids* **20**, art. 18203 (2018).

6. Anovitz L. M., Cole D. R., *Reviews in Mineralogy and Geochemistry* **80**, 61 (2015).

7. Barrie P. J., *Annual Reports on NMR Spectroscopy* **41**, 265 (2000).

8. Klochkov A., Tagirov M., *Low Temperature Physics* **41**, 50 (2015).

9. Lu Y., Liu K., Wang Y., *Applied Sciences* **11**, 8027 (2021).

10. Gazizulin R., Klochkov A., Kuzmin V., Safiullin K., Tagirov M., Yudin A., *Magnetic Resonance in Solids* **11**, 33 (2009).

11. Gizatullin B., Savinkov A., Shipunov T., Melnikova D., Doroginitzky M., Skirda V., *Magnetic Resonance in Solids* **20**, art. 18102 (2018).

12. Kenyon W., *The Log Analyst* **38**, 21 (1997).

13. Kleinberg R. L., Horsfield M. A., *Journal of Magnetic Resonance* **88**, 9 (1990).

14. Sigal R. F., *SPE Journal* **20**, 824 (2015).

15. Morales-Chávez S., Valdez-Grijalva M., Díaz-Viera M., Lucas-Oliveira E., Bonagamba T., *Journal of Magnetic Resonance* **379**, 107922 (2025).

16. Ghomeshi S., Kryuchkov S., Kantzas A., *Journal of Magnetic Resonance* **289**, 79 (2018).

17. Stepišnik J., Ardelean I., Mohorič A., *Journal of Magnetic Resonance* **328**, 106981 (2021).

18. Mutina A. R., Skirda V. D., *Journal of Magnetic Resonance* **188**, 122 (2007).

19. Hürlimann M. D., *Journal of Magnetic Resonance* **148**, 367 (2001).

20. Hürlimann M. D., Venkataramanan L., *Journal of Magnetic Resonance* **157**, 31 (2002).

21. Dullien F. A., *Porous media: fluid transport and pore structure* (Academic press, 2012).

22. Zhao P., Wang L., Xu C., Fu J., Shi Y., Mao Z., Xiao D., *Marine and Petroleum Geology* **111**, 66 (2020).

23. Rogozin A., Ignateva T., Churkov A., *Exposition Oil Gas* **6**, 62 (2021), [in Russian].

24. Wampler J., Rai C., Abdelghany O., in *SEG Technical Program Expanded Abstracts*, Vol. 29 (Society of Exploration Geophysicists, 2010) pp. 2649–2653.

25. Wang H., Ni W., Yuan K., Nie Y., Li L., *Bulletin of Engineering Geology and the Environment* **82**, 180 (2023).

26. Peesu R. R., Voleti D. K., Dutta A., Vanam P. R., Reddicharla N., in *Abu Dhabi International Petroleum Exhibition and Conference* (SPE, 2022) p. D012S145R004.

27. Fajt M., Machowski G., Puzio B., Krzyżak A. T., *Scientific Reports* **15**, 36688 (2025).

28. Strange J. H., Rahman M., Smith E., *Physical Review Letters* **71**, 3589 (1993).

29. Mitchell J., Webber J. B. W., Strange J. H., *Physics Reports* **461**, 1 (2008).

30. Petrov O., Furó I., *Microporous and Mesoporous Materials* **138**, 221 (2011).

31. Rottreau T. J., Parlett C. M., Lee A. F., Evans R., *Microporous and Mesoporous Materials* **264**, 265 (2018).

32. Rottreau T. J., Parlett C. M., Lee A. F., Evans R., *Microporous and Mesoporous Materials* **274**, 198 (2019).

33. Terenzi C., Sederman A. J., Mantle M. D., Gladden L. F., *Journal of Magnetic Resonance* **299**, 101 (2019).

34. Song Y.-Q., *Concepts in Magnetic Resonance Part A: An Educational Journal* **18**, 97 (2003).

35. Foley I., Farooqui S., Kleinberg R., *Journal of Magnetic Resonance* **123**, 95 (1996).

36. Hürlimann M. D., *Journal of Magnetic Resonance* **131**, 232 (1998).

37. Al-Jawad S. N. A., Ahmed M. A., Saleh A. H., *Journal of Petroleum Exploration and Production Technology* **10**, 3157 (2020).

38. Doroginitskii M., Ivanov A., *"Spectrum of spin-spin relaxation times,"* (2024), certificate no. 2024617332 of the Russian Federation; Kazan Federal University.

39. Carr H. Y., Purcell E. M., *Physical Review* **94**, 630 (1954).

40. Strange J., Betteridge L., Mallett M., in *Magnetic Resonance in Colloid and Interface Science* (Springer, 2002) pp. 155–169.

41. Cutler D., Powles J., *Proceedings of the Physical Society* **82**, 1 (1963).

42. Ivanov D., Barskaya E., Skirda V., *Magnetic Resonance in Solids* **21**, art. 19201 (2019).

43. Song Y.-Q., Ryu S., Sen P. N., *Nature* **406**, 178 (2000).

44. Stejskal E., *The Journal of Chemical Physics* **43**, 3597 (1965).

45. Mohnke O., Klitzsch N., *Vadose Zone Journal* **9**, 846 (2010).

46. Daigle H., Johnson A., Thomas B., *Geophysics* **79**, D425 (2014).

47. Petrov O. V., Furó I., *Progress in Nuclear Magnetic Resonance Spectroscopy* **54**, 97 (2009).